Journal of Power Sources 248 (2014) 553–559

Contents lists available at ScienceDirect

Journal of Power Sources

journal homepage: www.elsevier.com/locate/jpowsour

One-step and rapid synthesis of porous Pd nanoparticles with superior catalytic activity toward ethanol/formic acid electrooxidation

Wei Hong [a,b], Youxing Fang [a,b], Jin Wang [a,c,*], Erkang Wang [a,b,*]

[a] State Key Laboratory of Electroanalytical Chemistry, Changchun Institute of Applied Chemistry, Chinese Academy of Sciences, Changchun 130022, China
[b] University of Chinese Academy of Sciences, Beijing 100039, China
[c] Department of Chemistry and Physics, State University of New York at Stony Brook, New York, NY 11794-3400, USA

HIGHLIGHTS

- Porous Pd nanoparticles have been synthesized by a simple method.
- The developed method is efficient, rapid and convenient.
- Hydroquinone was used as the reductant to obtain porous Pd nanoparticles.
- The as-prepared catalysts exhibit excellent electrocatalytic activity.

ARTICLE INFO

Article history:
Received 2 July 2013
Received in revised form
26 September 2013
Accepted 29 September 2013
Available online 7 October 2013

Keywords:
Palladium
Porous
Catalytic activity
Ethanol
Formic acid
Electrooxidation

ABSTRACT

Porous Pd nanoparticles are successfully prepared by a rapid, one-step, and efficient route with high yield in aqueous solution. The developed method is very simple, just by mixing sodium tetrachloropalladate, polyvinylpyrrolidone and hydroquinone and heated at 70 °C for 15 min. The structure and composition are analyzed by transmission electron microscope, selected-area electron diffraction, inductively coupled plasma optical emission spectrometer, X-ray diffraction, energy dispersive X-ray spectrum and X-ray photoelectron spectroscopy. Electrochemical catalytic measurement results prove that the as synthesized porous Pd nanoparticles exhibit superior catalytic activity towards ethanol and formic acid electrooxidation.

1. Introduction

Palladium is an excellent and versatile catalyst in various important reactions, for example a large number of carbon–carbon bond forming reactions such as Suzuki, Heck, and Stille coupling [1–3]. It can also be served as electrode materials in direct fuel cells and attract increasing attention recently due to its remarkable performance [4,5]. Especially, different from its counterparts Pt, Pd catalyst does not suffer from the poison of C1 species such as CO_{ads} during the operation of direct ethanol fuel cells in alkaline media [6], and also own a lower oxidation overpotential towards formic acid electrooxidation [7]. The direct result is Pd catalyst shows an obvious better electrocatalytic performance than Pt during ethanol and formic acid electrooxidation reaction. However, Pd also occurs at very low levels of abundance in nature [3,5,8]. Therefore, further improvement of its catalytic activity and utilization efficiency by finely tuning the size, shape, composition are of highly importance [9–11]. The past few decades have witnessed the successful synthesis of Pd nanocrystals in a rich variety of shapes. In this regard, Pd nanocrystals with well defined structures, such as nanospheres [12,13], nanocubes [1,14,15], nanowires [16], nanotubes [17] and nanosheets [18], etc, have been synthesized.

Among these abundant materials, dendritic materials have been received much attention in the past few years. Because they are porous, their branches provide many high-index facets [19–21], and thus lead to the high performance during the catalysis. In the

* Corresponding authors. State Key Laboratory of Electroanalytical Chemistry, Changchun Institute of Applied Chemistry, Chinese Academy of Sciences, Changchun 130022, China. Fax: +86 43185689711.
E-mail addresses: jin.wang.1@stonybrook.edu (J. Wang), ekwang@ciac.jl.cn (E. Wang).

0378-7753/$ – see front matter © 2013 Elsevier B.V. All rights reserved.
http://dx.doi.org/10.1016/j.jpowsour.2013.09.126

past few years, pure Pt [22–24], Au@Pt core/shell [25], trimetallic Au@Pd@Pt Core/Shell [26,27], Pt-on-Pd [19,28], dendritic nanoparticles (NPs) have been prepared chemically. All of these dendritic materials presenting outstanding electrocatalytic activity. Therefore controlled synthesis of Pd nanostructure with porous shape is an attractive approach to achieve high catalytic performance. In this regard, several groups reported the successful synthesis of porous or dendritic Pd NPs. Yan's group [21] developed a seed mediated route to synthesize porous Pd nanoparticles (Pd PNPs), but the two-stepped process is slightly complicated. A few groups [29,30] employed hydrazine hydrates acting as the reductant to obtain porous palladium nanospheres, but hydrazine hydrates is highly toxic which should try to avoid the usage. Meng's group [31] reported a ultrasonic route to synthesize porous Pd nanospheres for formic acid electrooxidation. However the process is complicated and needs finely operating skills. The two-stepped reaction first treated K_2PdCl_4 and ascorbic acid in the ice-water bath for 5 min, and further proceeded 7 min in ultrasonic cleaner at 40 °C. Moreover, morphology of the final products was sensitive to the temperature and ultrasound power. Very recently, Yu and his co-workers [32] reported a method to prepare Pd PNPs in an organic mixture containing oleic acid and oleylamine. But the obtained Pd PNPs need a long time to clean the adsorbed organic molecules on the surface. Thus, the simple and rapid synthesis of Pd PNPs with high electrocatalytic activity is still highly desired and technologically important.

In this work, we propose a very simple, rapid, one-step, and efficient route to synthesize Pd PNPs with high yield in aqueous solution. The prepared Pd PNPs exhibit superior electro-catalytic activity for ethanol and formic acid electrooxidation reaction. In a typical synthesis, sodium tetrachloropalladate, polyvinylpyrroli done (PVP) and hydroquinone were mixed into an aqueous solution and heated at 70 °C for only 15 min. The obtained Pd PNPs were characterized by transmission electron microscopy (TEM), selected-area electron diffraction (SAED), inductively coupled plasma optical emission spectrometer (ICP-OES), X-ray diffraction (XRD), energy dispersive X-ray spectrum (EDS) and X-ray photoelectron spectroscopy (XPS). The catalytic activity and stability of the prepared catalysts toward ethanol and formic acid electrooxidation were investigated by cyclic voltammetry and chronoamperometry methods.

2. Experimental

2.1. Materials

Polyvinylpyrrolidone (PVP•K30, molecular weight: 50000–58000) and hydroquinone (HQ) were obtained from Beijing Chemical Corp (China). Vulcan XC-72 carbon was bought from Shanghai Ouman Chemical Corp (Shanghai, China). Commercial Pd/C (20% on activated carbon powder) and sodium tetrachloro palladate (II) were purchased from Alfa Asear. All chemicals used were of analytical grade and used without further purification. Milli-Q ultrapure water (Millipore, ≥18.2 MΩ cm) was used throughout the experiments.

2.2. Preparation of porous Pd nanoparticles

70 μL Na_2PdCl_4 (0.06 mol L^{-1}) together with 20 mg PVP (K 30) were mixed into 15 mL water and stirred to form a homogeneous solution. After that, 1 mL HQ (0.03 mol L^{-1}) was quickly injected to the mixture and sequentially heated at 70 °C for 15 min. The products were collected via centrifugation at 10000 rpm for 15 min and further washed several times by water.

2.3. Preparation of carbon supported porous Pd nanoparticles

1.5 mg Vulcan XC-72 carbon were mixed with the prepared porous Pd nanoparticles and sonicated for 15 min, then stirred for 10 h. Finally, the products were collected by centrifugation.

2.4. Material structure and composition characterizations

Transmission electron microscopy (TEM), high-resolution transmission electron microscopy (HRTEM) measurements, SAED and EDS were made on a JEM-2100F high-resolution transmission electron microscope operating at 200 kV. The composition of Pd PNPs was determined by inductively coupled plasma-mass spectroscopy (ICP-MS, X Series 2, Thermo Scientific USA). XRD pattern of the as prepared Pd nanoparticles was recorded on a D8 ADVANCE (BRUKER, Germany) diffractometer using Cu–Kα radiation with a Ni filter ($\lambda = 0.154059$ nm at 30 kV and 15 mA). XPS measurement was performed on an ESCALAB-MKII spectrometer (VG Co., United Kingdom) with Al Kα X-ray radiation as the X-ray source for excitation.

2.5. Electrochemical catalytic test toward ethanol/formic acid electrooxidation

Electrochemical experiments were performed with a CHI 832B electrochemical workstation (Chenhua Instruments Corp, Shanghai, China). A conventional three-electrode cell was used, including an Ag/AgCl (saturated KCl) electrode as reference electrode, a platinum wire as counter electrode and modified glassy carbon electrode as working electrode respectively. Before each experiment, the GCE was polished carefully with 1.0, 0.3, and 0.05 μm alumina powder and rinsed with deionized water, followed by sonication in ethanol and Milli-Q ultrapure water successively. Then, the electrode was dried under nitrogen. For electrooxidation test, 5 μL of commercial Pd/C or carbon supported porous Pd nanoparticles catalysts solution (0.5 mg mL^{-1} of metal) was dropped on the surface of the GC electrode and dried with an infrared lamp carefully. Then, 5 μL of Nafion (0.5%) was coated on the surface of the above material modified GCE and dried before electrochemical experiments.

3. Results and discussion

3.1. TEM, SAED and ICP-OES characterizations of the Pd PNPs catalysts

The morphology and structure of the as-synthesized samples were characterized by transmission electron microscopy (TEM). Fig. 1a, c, d shows the typical TEM images of the prepared Pd PNPs with different magnification. Fig. 1a and b obviously show that the entire resulting samples are definitely endowed with porous morphology, indicating the high yield production of Pd PNPs. Fig. 1b presents the size distribution of the prepared Pd PNPs. The average size of the particles is about 32.5 nm. The high-resolution TEM (HRTEM) image shows that the Pd PNPs are in the polycrystalline state, of which the d spacing is 0.226 nm, which can be assigned to the (111) planes of Pd (Fig. 1e). The selected area electron diffraction patterns of one single porous Pd nanoparticles is depicted in Fig. 1f. There are four bright concentric rings that attributed to (111), (200), (220) and (311) planes of Pd respectively, which further confirm that the Pd PNPs are polycrystalline. Fig. 2 A shows the XRD pattern of Pd PNPs. Three characteristic diffraction peaks at 40.1°, 46.6° and 68.1°, which assigned to Pd (111), Pd (200) and Pd (220) planes respectively can be observed, matching the standard pattern of pure Pd (JCPDS No.65–2867) well. Fig. 2C presents the EDS of the

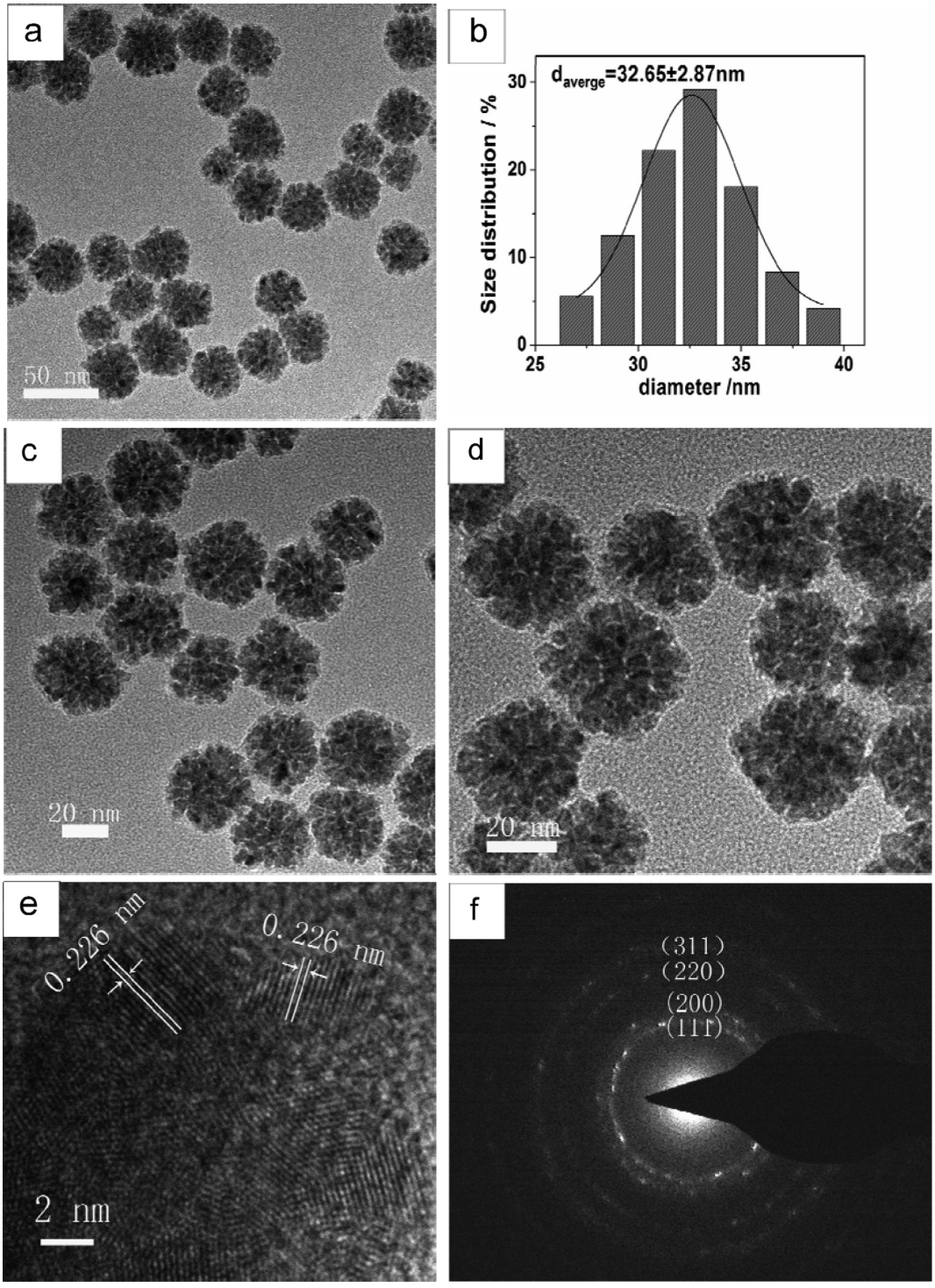

Fig. 1. (a, c, d) Typical TEM images of the prepared porous Pd nanoparticles with different magnification. (b) Size distribution of the prepared Pd nanoparticles. (e) High-resolution TEM images. (f) Selected-area electron diffraction of a single prepared porous Pd nanoparticles.

prepared Pd PNPs, the peak of Pd can be noted obviously, while the peak of Cu and C element were originated from the carbon coated copper grid. The XPS pattern (Fig. 2B) of the resulting Pd PNPs shows significant Pd 3d signals corresponding to the binding energy of Pd, which also indicates that the obtained nanostructures were exclusively composed of pure palladium.

It is well known that HQ has a weak reducing ability with reduction potential ($E^\circ = -0.699$ vs NHE) [33,34], and it is commonly used to selectively reduce silver because it is unable to spontaneously reduce Ag^+ ions that are isolated in solution (Ag^+/Ag^0, $E^\circ = -1.8$ V) but can reduce Ag^+ in the presence of Ag^0 clusters or nanoparticles ($E^\circ = +0.799$ V) [35]. And its weak reducing ability has also been applied to synthesize highly monodispersed, spherical gold nanoparticles of 50–200 nm [34]. However, rare reports appeared about the use of HQ to synthesize well–defined nanocrystals of Pd or Pt in aqueous solution. In this manuscript, we

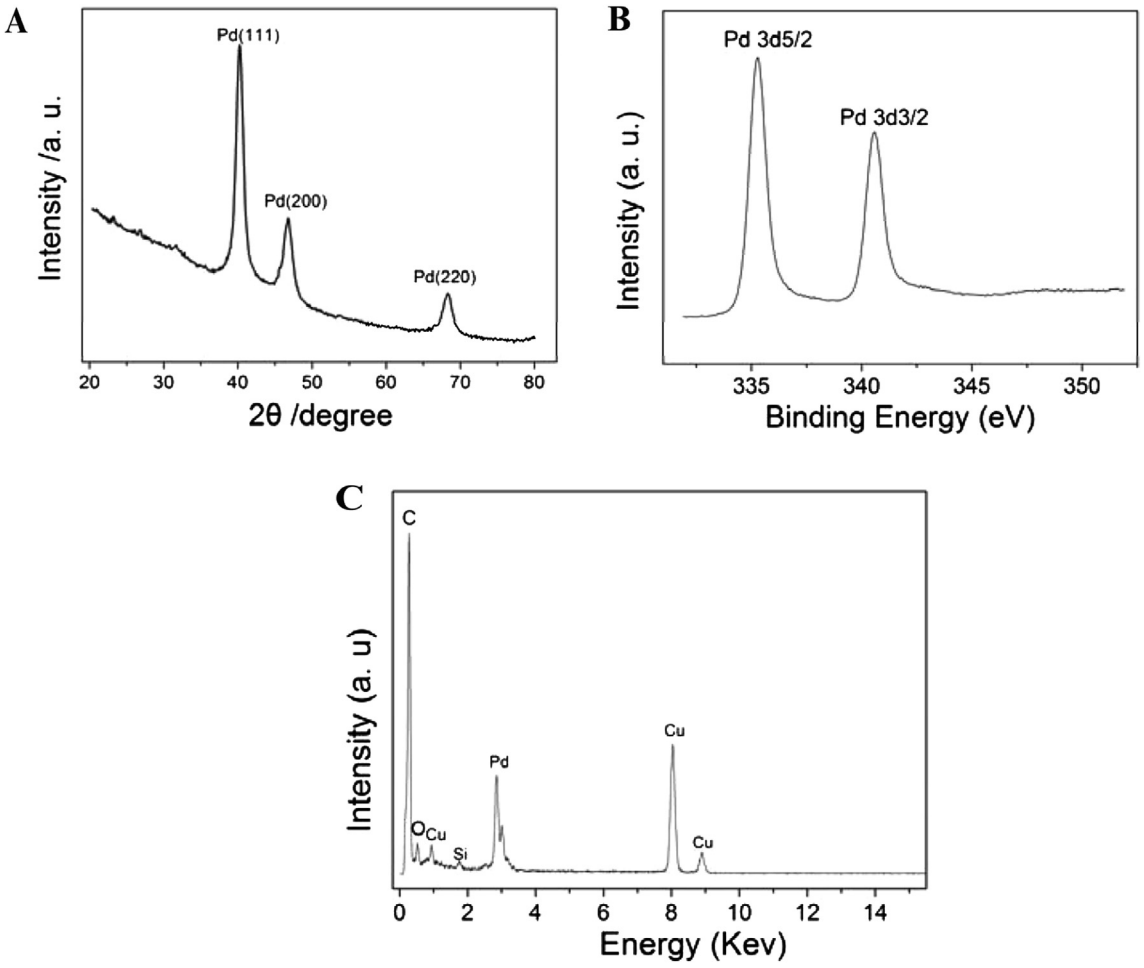

Fig. 2. (A) XRD pattern of the prepared porous Pd nanoparticles. (B) XPS pattern of the prepared porous Pd nanoparticles. (C) EDS of the prepared porous Pd nanoparticles.

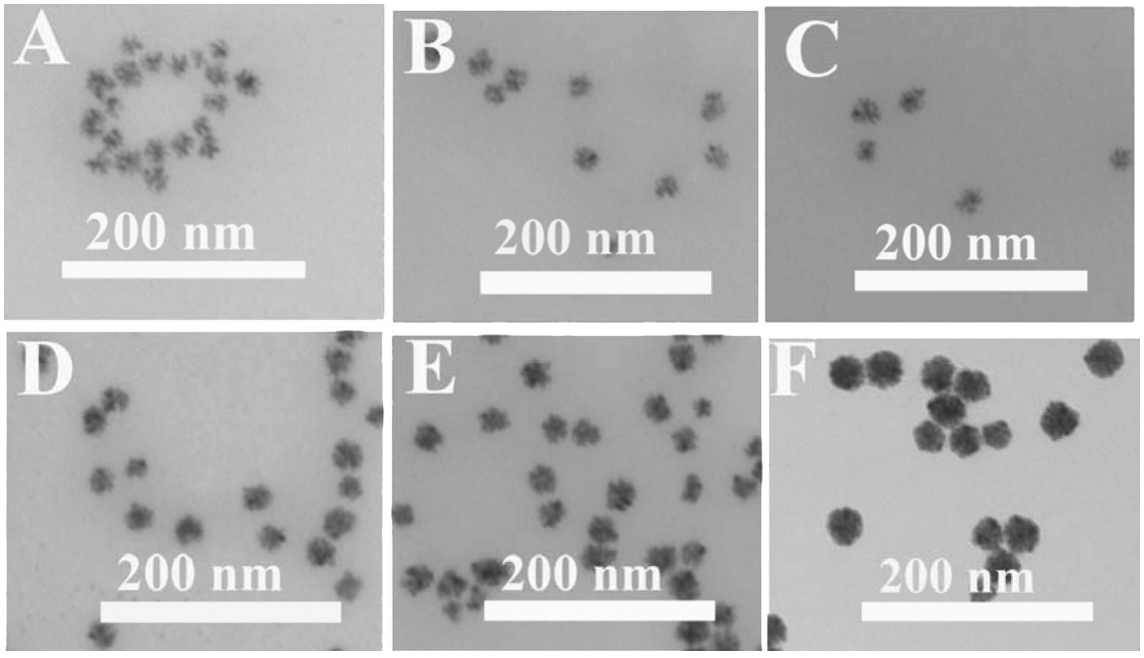

Fig. 3. TEM images of the intermediate products collected at different reaction times, (A) 5, (B) 7, (C) 9, (D) 11, (E) 13 and (F) 15 min, respectively.

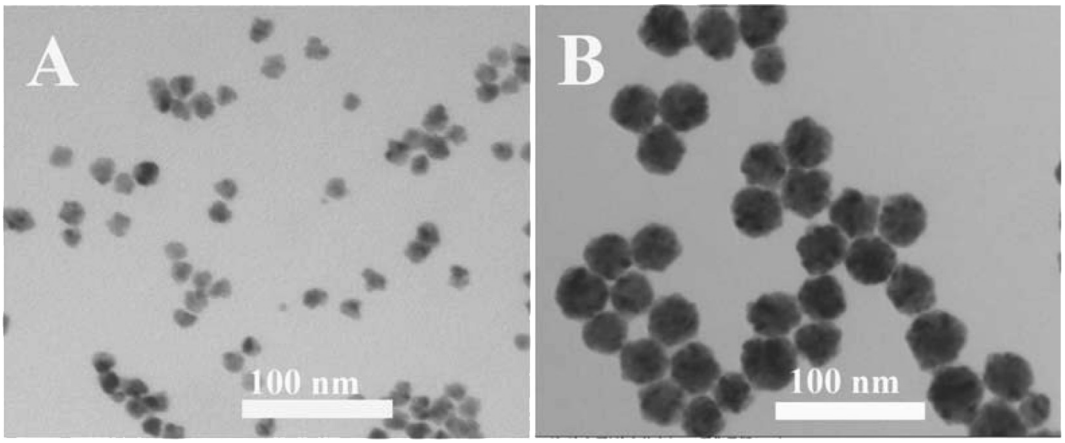

Fig. 4. TEM images of the products synthesized from different concentration of Pd precursor, (A) 15 μL 0.06 mol L^{-1} Na_2PdCl_4 (B) 350 μL 0.06 mol L^{-1} Na_2PdCl_4.

pioneered to use HQ as the reductant to obtain Pd PNPs. In order to figure out the possible mechanism of the formation of Pd PNPs, the intermediate products at different time intervals were collected and characterized by TEM (Fig. 3). The results demonstrate that this type of Pd nanostructures is a result of epitaxial growth of initially formed small palladium NPs rather than an aggregated growth mode, which can be reasonably attributed to the slow and continuous nucleation deriving from the relatively weak reducing power of HQ, and autocatalytic growth [24,36–39]. The influence of reaction temperature was investigated. As the temperature increased, the reaction rate increased correspondingly, and thus led to the decrease of the monodispersity of the final products (data not shown). The concentration of Pd precursors had a slight influence on the morphology of the final products (Fig. 4), the higher precursor concentration resulted in larger size of the final products.

To evaluate the catalytic activity of the prepared Pd PNPs, Vulcan XC-72 carbon were used to support the Pd PNPs, TEM image can be found in Fig. 5. The content of Pd in the carbon supported Pd PNPs was determined by ICP-OES, the mass fraction of Pd is 22%.

3.2. Electrochemical measurements of carbon supported Pd PNPs and commercial Pd/C catalysts

The catalytic activity of the carbon supported porous Pd nanoparticles (VXC-Pd PNPs) towards ethanol and formic acid electrooxidation were carried out with an electrochemical measurement system, and further compared with a commercial Pd/C catalyst. Specific activity was used to evaluate the catalytic activity of the prepared catalyst. Fig. 6 shows the cyclic voltammetry curve of commercial Pd/C catalyst and VXC-Pd PNPs modified glassy carbon electrode in a N_2–saturated 0.5 mol L^{-1} H_2SO_4 solution at the scan rate of 50 mV s^{-1}. On the basis of the assumption that the charge density for the formation of a fully covered $Pd(OH)_2$ monolayer was 430 μC cm^{-2} [40], the electrochemically active surface area (ECSA) of the catalyst can be estimated. The ECSA of VXC-Pd PNPs is 43.8 m^2 g^{-1}, lower than 49.2 m^2 g^{-1} of commercial Pd/C. Current density was normalized to ECSA estimated from the reduction charge of the $Pd(OH)_2$. Electrooxidation towards ethanol was carried out in an aqueous solution containing 0.5 mol L^{-1} sodium hydroxide and 1 mol L^{-1} ethanol, using cyclic voltammetry (CV) measurement technique, sweeping from −0.8 V to 0.4 V at a scan rate of 50 mV s^{-1}. Fig. 7a shows the specific activity of the two catalyst towards ethanol electrooxidation. The forward anodic peak

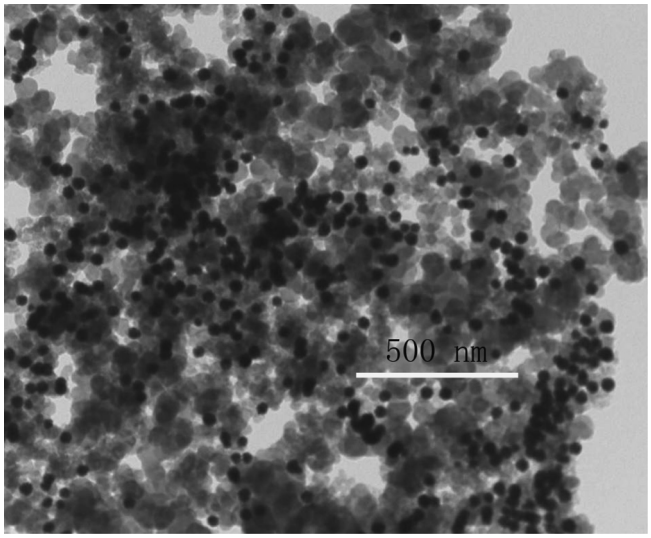

Fig. 5. Typical TEM images of Vulcan XC-72 carbon supported porous Pd nanoparticles.

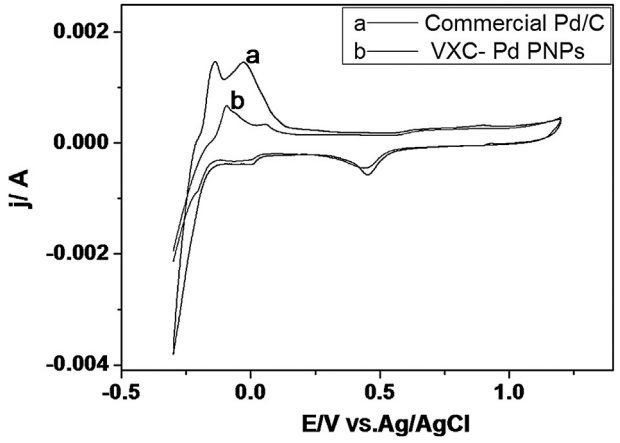

Fig. 6. Cyclic voltammetry curve of commercial Pd/C catalyst and porous Pd supported on Vulcan XC-72 carbon modified glassy carbon electrode in a N_2-sparged 0.5 mol L^{-1} H_2SO_4 solution at the scan rate of 50 mV s^{-1}. The loading metal of Pd of each catalyst is 25.1 μg cm^{-2}.

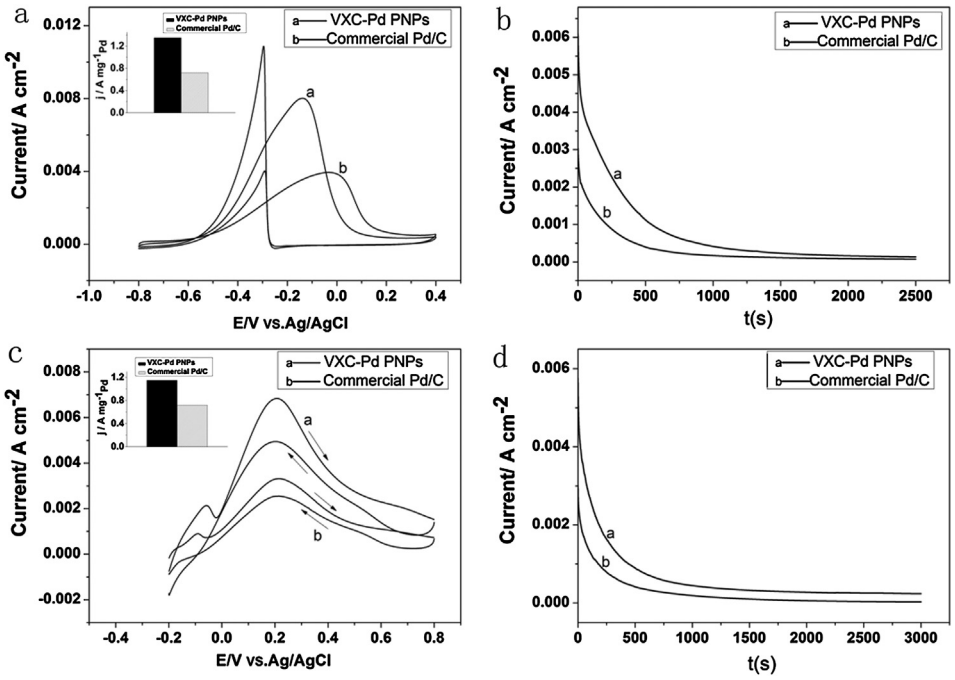

Fig. 7. (a) Specific activity towards ethanol electrooxidation in a solution containing 1 mol L^{-1} ethanol + 0.5 mol L^{-1} sodium hydroxide at a scan rate of 50 mV s^{-1}, the inset histogram is the mass activity towards ethanol electrooxidation recorded at −0.14 V. (b) Current-time curve recorded at −0.2 V in a solution containing 1 mol L^{-1} ethanol + 0.5 mol L^{-1} sodium hydroxide. (c) Specific activity towards formic acid electrooxidation in a solution containing 0.5 mol L^{-1} HCOOH + 0.5 mol L^{-1} H_2SO_4 at a scan rate of 50 mV s^{-1}, the inset histogram is the mass activity towards formic acid electrooxidation recorded at 0.2 V. (d) Current-time curve recorded at 0.2 V in solution containing 0.5 mol L^{-1} HCOOH + 0.5 mol L^{-1} H_2SO_4.

value of specific activity for VXC-Pd PNPs catalyst is 8.1 mA cm^{-2}, which is 1.96 times higher than 4.15 mA cm^{-2} of commercial Pd/C. The results is also better than PtPd bimetallic NPs on Nafion–graphene [41] The inset histogram in Fig. 7a shows the mass activity of the prepared catalyst and commercial Pd/C towards ethanol electrooxidation recorded at −0.14 V, the mass activity of VXC-Pd NPs is about 1.8 times higher than the commercial Pd/C. The result further confirms that prepared Pd PNPs possess an excellent catalytic activity toward ethanol electrooxidation in alkaline condition. It can also be noted from Fig. 7a that the anodic peak ethanol electrooxidation potential of VXC-Pd NPs in the forward scan is at −0.14 V, which shifts negatively to 0.12 V compared to the commercial Pd/C that is 0.02 V. The decrease in the onset anodic potential indicates the enhancement in the kinetics of the ethanol oxidation reaction. The stability of VXC-Pd PNPs towards ethanol electrooxidation was investigated by current-time method (Fig. 7b). The current decay for the reaction on the VXC-Pd PNPs is slower than commercial Pd/C electrocatalysts, indicating that the VXC-Pd PNPs possess the superior electrochemical stability for ethanol electrooxidation in alkaline media. After about 1500 s, both VXC-Pd PNPs and commercial Pd/C show a sharp decrease current value. The phenomenon might be attributed to the formation of the oxide layer on the surface of electrode which can block the adsorption of the reactive species onto the Pd surface and lead to a decrease in the electrocatalytic activity [42]. It is generally believed that a CH_3CO_{ads} intermediate is formed on the Pd catalyst in the alkaline medium, and its reaction with OH_{ads} is the rate-determining step [42].

Similarly, electrooxidation towards formic acid was carried out in an aqueous solution containing 0.5 mol L^{-1} formic acid and 0.5 mol L^{-1} sulfuric acid, using CV technique, sweeping from −0.2 V to 0.8 V at a scan rate of 50 mV s^{-1}. The forward anodic peak of VXC-Pd PNPs is 0.0068 A cm^{-2}, 1.9 times of commercial Pd/C of 0.0035 A cm^{-2} as illustrated in Fig. 7c, indicating that the as prepared VXC-Pd PNPs possess an excellent catalytic activity. The result is also higher than 0.006 A cm^{-2} of Pt/Pd bimetallic nanotubes [43]. The mass activity of VXC-Pd PNPs recorded at 0.2 V was 1.15 A $mg^{-1}{}_{Pd}$, 1.5 times higher than commercial Pd/C of 0.74 A $mg^{-1}{}_{Pd}$ (inset histogram of Fig. 7c). Learned from Fig. 7c, it can also be found that the peak value in backward scan of VXC-Pd PNPs is 0.00496 A cm^{-2} and is also much higher than commercial Pd/C of 0.0027 A cm^{-2}. The stability of VXC-Pd PNPs towards formic acid electrooxidation was also investigated by chronoamperometry technique at 0.2 V and compared with commercial Pd/C electrocatalyst as illustrated in Fig. 7d. It can be clearly found that the current decay for formic acid electrooxidation reaction on the VXC-Pd PNPs is significantly slower than commercial Pd/C electrocatalyst. VXC-Pd PNPs show a distinct higher current value than commercial Pd/C during the 3000 s test. The results demonstrated that the as-prepared VXC-Pd PNPs has a good tolerance towards formic acid electrooxidation. All the results prove that VXC-Pd PNPs possess excellent catalytic activity towards formic acid electrooxidation.

4. Conclusions

In conclusion, we have successfully synthesized porous Pd nanoparticles through a very convenient one-step route, just by mixing sodium tetrachloropalladate, polyvinylpyrrolidone and hydroquinone and heated at 70 °C for 15 min. The developed method is very simple, rapid and efficient. The as prepared catalyst shows excellent catalytic activity towards ethanol and formic acid electrooxidation, which is better than the commercial Pd/C, presenting wide potential application for direct fuel cells in the future.

Acknowledgments

The authors acknowledge the financial support of National Natural Science Foundation of China with Grant Nos. 21190040, 91227114 and 973 projects (Nos. 2010CB933600).

References

[1] Y. Xiong, Y. Xia, Adv. Mater. 19 (2007) 3385–3391.
[2] B. Lim, M. Jiang, J. Tao, P.H.C. Camargo, Y. Zhu, Y. Xia, Adv. Funct. Mater. 19 (2009) 189–200.
[3] S. Cheong, J.D. Watt, R.D. Tilley, Nanoscale 2 (2010) 2045–2053.
[4] C. Bianchini, P.K. Shen, Chem. Rev. 109 (2009) 4183–4206.
[5] S. Sun, Z. Jusys, R.J. Behm, J. Power Sources 231 (2013) 122–133.
[6] S.C. Lai, M.T. Koper, Phys. Chem. Chem. Phys. 11 (2009) 10446–10456.
[7] X. Wang, J. Yang, H. Yin, R. Song, Z. Tang, Adv. Mater. 25 (2013) 2728–2732.
[8] E. Antolini, Energy Environ. Sci. 2 (2009) 915–931.
[9] B. Wu, N. Zheng, Nano Today 8 (2013) 168–197.
[10] J.W. Hong, D. Kim, Y.W. Lee, M. Kim, S.W. Kang, S.W. Han, Angew. Chem. Int. Ed. 50 (2011) 8876–8880.
[11] Z.Y. Zhou, Z.Z. Huang, D.J. Chen, Q. Wang, N. Tian, S.G. Sun, Angew. Chem. Int. Ed. 49 (2010) 411–414.
[12] M. Cargnello, N.L. Wieder, P. Canton, T. Montini, G. Giambastiani, A. Benedetti, R.J. Gorte, P. Fornasiero, Chem. Mater. 23 (2011) 3961–3969.
[13] M. Moreno, F.J. Ibanez, J.B. Jasinski, F.P. Zamborini, J. Am. Chem. Soc. 133 (2011) 4389–4397.
[14] W. Niu, L. Zhang, G. Xu, ACS Nano 4 (2010) 1987–1996.
[15] W. Niu, Z.-Y. Li, L. Shi, X. Liu, H. Li, S. Han, J. Chen, G. Xu, Crystal Growth Des. 8 (2008) 4440–4444.
[16] X. Huang, N. Zheng, J. Am. Chem. Soc. 131 (2009) 4602–4603.
[17] M.A. Lim, D.H. Kim, C.-O. Park, Y.W. Lee, S.W. Han, Z. Li, R.S. Williams, I. Park, ACS Nano 6 (2011) 598–608.
[18] P.F. Siril, L. Ramos, P. Beaunier, P. Archirel, A. Etcheberry, H. Remita, Chem. Mater. 21 (2009) 5170–5175.
[19] B. Lim, M. Jiang, P.H. Camargo, E.C. Cho, J. Tao, X. Lu, Y. Zhu, Y. Xia, Science 324 (2009) 1302–1305.
[20] B. Lim, Y. Xia, Angew. Chem. Int. Ed. 50 (2011) 76–85.
[21] F. Wang, C. Li, L.D. Sun, C.H. Xu, J. Wang, J.C. Yu, C.H. Yan, Angew. Chem. Int. Ed. 51 (2012) 4872–4876.
[22] L. Wang, C. Hu, Y. Nemoto, Y. Tateyama, Y. Yamauchi, Crystal Growth Des. 10 (2010) 3454–3460.
[23] L. Wang, Y. Yamauchi, Chem. Mater. 21 (2009) 3562–3569.
[24] L. Wang, H. Wang, Y. Nemoto, Y. Yamauchi, Chem. Mater. 22 (2010) 2835–2841.
[25] H. Ataee-Esfahani, L. Wang, Y. Yamauchi, Chem. Commun. 46 (2010) 3684–3686.
[26] L. Wang, Y. Yamauchi, Chem. Mater. 23 (2011) 2457–2465.
[27] L. Wang, Y. Yamauchi, J. Am. Chem. Soc. 132 (2010) 13636–13638.
[28] L. Wang, Y. Nemoto, Y. Yamauchi, J. Am. Chem. Soc. 133 (2011) 9674–9677.
[29] G. Fu, W. Han, L. Yao, J. Lin, S. Wei, Y. Chen, Y. Tang, Y. Zhou, T. Lu, X. Xia, J. Mater. Chem. 22 (2012) 17604–17611.
[30] L. Wang, E. Tan, L. Guo, X. Han, Nanotechnology 22 (2011) 305712.
[31] S. Tang, S. Vongehr, Z. Zheng, H. Ren, X. Meng, Nanotechnology 23 (2012) 255606.
[32] Q. Gao, M.R. Gao, J.W. Liu, M.Y. Chen, C.H. Cui, H.H. Li, S.H. Yu, Nanoscale 5 (2013) 3202–3207.
[33] S.T. Gentry, S.J. Fredericks, R. Krchnavek, Langmuir 25 (2009) 2613–2621.
[34] S.D. Perrault, W.C.W. Chan, J. Am. Chem. Soc. 131 (2009) 17042–17043.
[35] T. Linnert, P. Mulvaney, A. Henglein, H. Weller, J. Am. Chem. Soc. 112 (1990) 4657–4664.
[36] E.P. Lee, J. Chen, Y. Yin, C.T. Campbell, Y. Xia, Adv. Mater. 18 (2006) 3271–3274.
[37] J. Chen, T. Herricks, M. Geissler, Y. Xia, J. Am. Chem. Soc. 126 (2004) 10854–10855.
[38] E.P. Lee, Z. Peng, W. Chen, S. Chen, H. Yang, Y. Xia, ACS Nano 2 (2008) 2167–2173.
[39] E.P. Lee, Y. Xia, Nano Res. 1 (2008) 129–137.
[40] L. Xiao, L. Zhuang, Y. Liu, J. Lu, H. Abruna, J. Am. Chem. Soc. 131 (2009) 602–608.
[41] X. Yang, Q. Yang, J. Xu, C.-S. Lee, J. Mater. Chem. 22 (2012) 8057–8062.
[42] Z.X. Liang, T.S. Zhao, J.B. Xu, L.D. Zhu, Electrochim. Acta 54 (2009) 2203–2208.
[43] S. Guo, S. Dong, E. Wang, Energy Environ. Sci. 3 (2010) 1307–1310.